Journal of Bone Oncology 18 (2019) 100256

Contents lists available at ScienceDirect

Journal of Bone Oncology

journal homepage: www.elsevier.com/locate/jbo

Research Paper

Intra-articular osteoid osteoma accompanied by extensive bone marrow edema. A clinical and micro-morphological analysis

Tim Rolvien[a,b,*], Matthias Krause[a,c], Jozef Zustin[a,d], Oleg Yastrebov[e], Ralf Oheim[a], Florian Barvencik[a], Karl-Heinz Frosch[c], Michael Amling[a,**]

[a] Department of Osteology and Biomechanics, University Medical Center Hamburg-Eppendorf, Hamburg, Germany
[b] Department of Orthopedics, University Medical Center Hamburg-Eppendorf, Hamburg, Germany
[c] Department of Trauma, Hand and Reconstructive Surgery, University Medical Center Hamburg-Eppendorf, Hamburg, Germany
[d] Pathologisch-Anatomisches Institut Regensburg, Regensburg, Germany
[e] Department of Foot Surgery, Agaplesion Diakonieklinikum, Hamburg, Germany

ARTICLE INFO

Keywords:
Osteoid osteoma
Bone marrow edema
Joint pain
Bone tumor
MRI
qBEI

ABSTRACT

Osteoid osteoma (OO) is a benign bone tumor producing non-mineralized bone matrix (i.e., osteoid). While peritumoral edema is commonly found in OO, extensive bone marrow edema has been reported less frequently. Furthermore, the micro-morphological characteristics of the nidus and its central calcification remain unclear. In this study, a consecutive series of four patients suffering from extensive bone marrow edema triggered by intra-articular osteoid osteoma underwent clinical examination, magnetic resonance imaging (MRI) and computed tomography (CT) as well as dual-energy X-ray absorptiometry (DXA) and laboratory bone turnover analyses. The obtained resection specimens were processed by undecalcified histology and were subsequently analyzed by light microscopy and quantitative backscattered electron imaging (qBEI). We report an entity of intra-articular osteoid osteoma in the knee and foot, in which an extensive and persistent bone marrow edema syndrome masked the correct diagnosis. While metabolic bone diseases were excluded in all cases, the reassessment of the patients' clinical history including pain characteristics (nocturnal, aspirin sensitivity) led us to perform additional CT, where the tumor was diagnosed. The micro-morphological analysis of the OO biopsies revealed that the nidus was surrounded by hyperosteoidosis, while central mineralization was detected in all cases. This mineralized area showed a significantly higher mineralization heterogeneity than the surrounding trabecular bone and more disorganized collagen fibers detected by qBEI and polarized light microscopy, respectively. Taken together, our results indicate that osteoid osteoma should be considered when persistent and extensive, peri-articular bone marrow edema is diagnosed. The central calcification that is found inside the nidus in conventional imaging was mirrored by bone matrix with a heterogeneous mineralization pattern.

1. Introduction

Osteoid osteoma (OO) represents a benign bone tumor that produces unmineralized bone called osteoid. Regarding its imaging appearance in magnetic resonance imaging (MRI) and/or computed tomography (CT), this area of osteoid is called nidus, while a central area of calcification is usually also visible [1,2]. OO typically affects the long bones or vertebrae of adolescents or young adults but also atypical locations have been reported [3,4]. OO may be localized cortically, trabecularly or subchondrally/ intra-articularly [2,3,5]. Next to the nidus, nocturnal pain that responds to nonsteroidal anti-inflammatory drugs (NSAIDs), especially salicylates, represents the most prominent clinical feature of OO [6]. On a molecular level, it was previously shown that OO have an oncogenic structural rearrangement in the AP-1 transcription factor (either FOS or FOSB) [7,8].

Intra-articular osteoid osteoma was previously reported as an important differential diagnosis for joint pain [3], which is initially often assigned to more common differential diagnoses including inflammatory joint diseases or osteochondritis dissecans [3,9]. Although it is known that benign and malignant bone tumors can be associated with bone marrow edema detected by MRI, bone marrow edema may be another relevant reason for the initial incorrect diagnosis. In fact, misdiagnosis of OO due to bone marrow edema was previously reported [10]. On the other hand, the occurrence of a distinct bone marrow

* Corresponding author at: Department of Osteology and Biomechanics, University Medical Center Hamburg-Eppendorf, Lottestr. 59, 22529 Hamburg, Germany.
** Corresponding author.
E-mail addresses: t.rolvien@uke.de (T. Rolvien), amling@uke.de (M. Amling).

https://doi.org/10.1016/j.jbo.2019.100256
Received 5 June 2019; Received in revised form 16 August 2019; Accepted 19 August 2019
Available online 20 August 2019

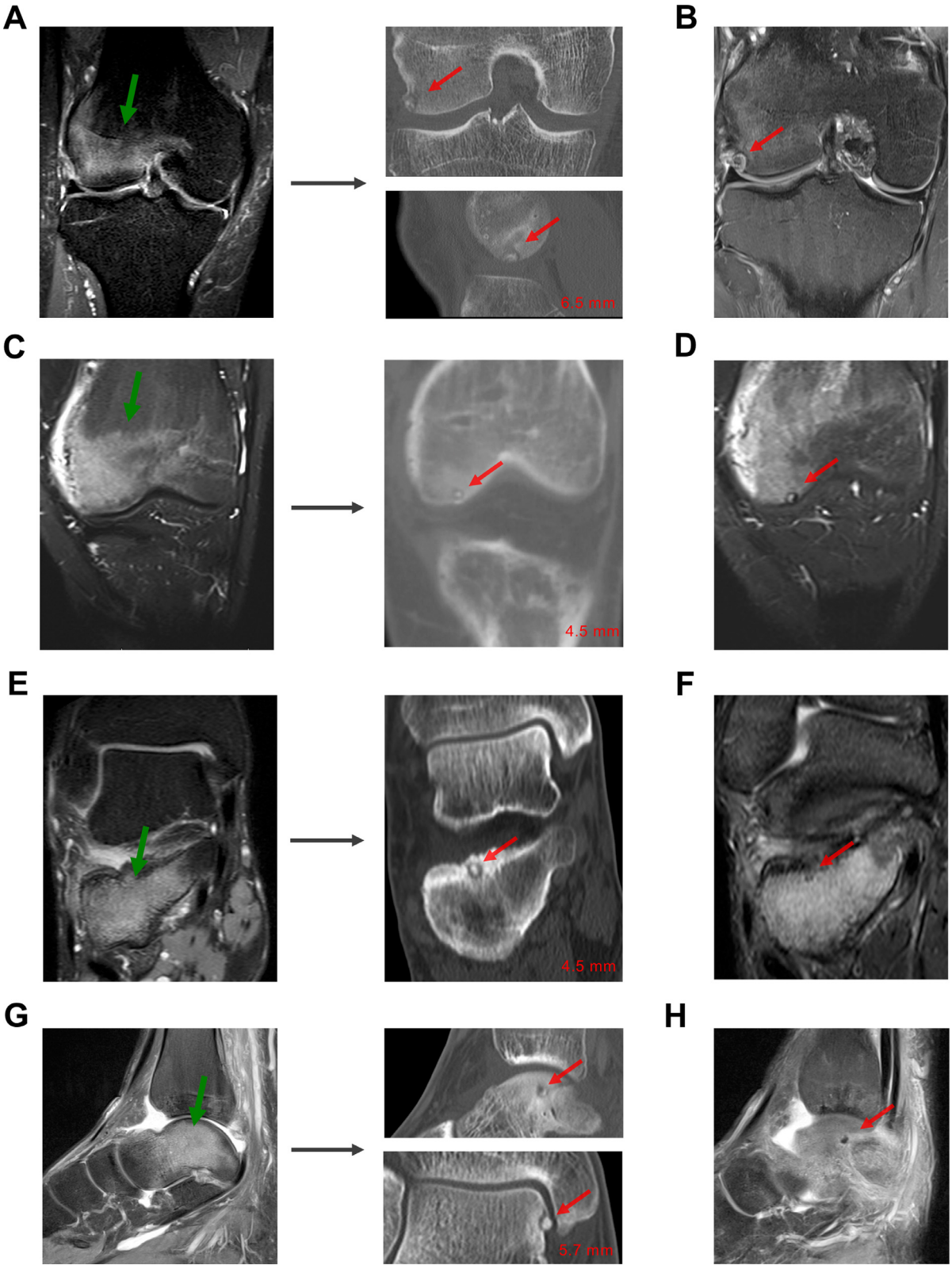

Fig. 1. *Extensive bone marrow edema as a presentation of intra-articular osteoid osteoma in different joints.* (A) Coronal proton density MRI sequence showing the bone marrow edema of the lateral femur condyle (green arrow) in *Case 1* and subsequent CT scan unmasking a nidus (red arrow). Right lower corner: Nidus diameter. (B) Identification of the nidus at MRI re-examination. Coronal proton density fat-saturated MRI sequence. (C) Extensive bone marrow edema of the lateral femur condyle (green arrow) in *Case 2* and CT scan showing a small nidus (red arrow). (D) Coronal and sagittal T2-weighted fat-saturated MRI sequence. (E) Extensive bone marrow edema of the calcaneus (green arrow) in *Case 3* and nidus seen in coronal CT reformat (Red arrow). (F) Coronal and axial T2-weighted fat-saturated MRI sequence with suspect of a nidus. (G) Sagittal proton density MRI sequence showing the persistent bone marrow edema (green arrow) and joint effusion in *Case 4*. CT revealed a subchondral nidus pointing to osteoid osteoma (red arrow). Red arrows indicate the nidus. (H) Sagittal proton density fat-saturated MRI sequence. (For interpretation of the references to colour in this figure legend, the reader is referred to the web version of this article.)

Table 1
Laboratory values and DXA Z-scores in the lumbar spine and hip assessed by DXA.

Parameter	Case 1	Case 2	Case 3	Case 4	Reference range
Ca (mmol/l)	2.26	2.45	2.27	2.35	2.13–2.63
AP (U/l)	68	51	78	53	40–129
TSH (mU/l)	1.12	1.17	1.06	0.69	0.27–4.20
Gastrin (ng/l)	65	32	12 (-)	34	13–115
25-OH-D3 (μg/l)	37.9	19.1 (-)	15.0 (-)	23.7 (-)	>30
PTH (ng/l)	42.8	15.3 (-)	50.5	26.7	17–84
BAP (μg/l)	8.8	9.3	17.2	9.7	5.5–22.9
Osteocalcin (μg/l)	16.7	17.9	20.8	23.1	12–52.1
DPD (nmol/mmol)	5	2	5	4	2–5
DXA Z-score LS	0.5	0.7	0.1	−0.5	(−1)–(+1)
DXA Z-score hip	−0.2	0.5	−2.2	−0.8	(−1)–(+1)

Ca: calcium, AP: alkaline phosphatase, TSH: thyroid-stimulating hormone, 25-OH-D3: 25-hydroxyvitamin D3, PTH: parathyroid hormone, BAP: bone-specific alkaline phosphatase. DPD: deoxypyridinoline. (-) indicates low levels.

edema (i.e., half-moon appearance in the femoral neck) has been described as a highly sensitive and specific feature for the diagnosis of osteoid osteoma [11].

The aim of the present study was to determine the skeletal status of patients with extensive bone marrow edema due to late-diagnosed OO and to outline the micro-morphological characteristics of obtained OO specimens. While we outline extensive bone marrow edema as a reason for prolonged or misdiagnosis of osteoid osteoma, a full skeletal assessment was conducted in these patients in order to determine potential risk factors for the occurrence of extensive bone marrow edema in OO. Moreover, the mineral distribution of the nidus area containing a central calcification was assessed by quantitative backscattered electron imaging to find a potential correlate for the unique radiologic appearance of OO.

2. Methods

2.1. Patients

Four patients with extensive bone marrow edema are reported in this study. These patients (*Cases 1–4*) were 48, 22, 26, and 20 years of age. No specific risk factors for bone diseases were present in these patients. Magnetic resonance imaging (MRI) was followed by computed tomography (CT) to confirm the diagnosis. Informed consent was obtained from the patients.

2.2. Skeletal assessment

In order to further analyze the bone status, the areal bone mineral density (aBMD) was evaluated using Dual Energy X-Ray absorptiometry (DXA, Lunar iDXA, GE Healthcare; Madison, WI, USA). Furthermore, serum and urinary bone turnover markers including calcium, alkaline phosphatase (AP), thyroid-stimulating hormone (TSH), gastrin, 25-hydroxyvitamin D (25-OH-D_3), parathyroid hormone (PTH), bone-specific alkaline phosphatase (BAP), osteocalcin (Oc), and deoxypyridinoline cross-links in the urine (DPD) were assessed.

2.3. Biopsy studies

All biopsies were evaluated by a specialist bone pathologist to confirm the diagnosis of OO. Contact radiography was performed, and the specimens were subsequently fixed in 3.7% formaldehyde, dehydrated, embedded in methyl methacrylate, and cut on a Microtec rotation microtome (CVT 4060E, Micro Tec, Germany). Afterwards, the 5-μm sections were stained by toluidine blue, trichrome Masson-Goldner and von Kossa. The sections were analyzed using an Olympus BX-61 microscope (Olympus, Germany) equipped with polarized light filter sets.

The bone mineralization density distribution (BMDD) was assessed within the calcified/mineralized nidus as well as in the trabecular bone next to the tumor by quantitative backscattered electron imaging (*qBEI*, LEO 435 VP; LEO Electron Microscopy Ltd., Cambridge, England) [12]. The signal amplification was adjusted by reference to the mean signal level of carbon and aluminum standards (MAC Consultants Ltd., England). Four images per region of interest were obtained (100x magnification). The mean calcium content (CaMean) and the heterogeneity (CaWidth) of the calcium distribution were calculated and calcium distribution curves were calculated using ImageJ (ImageJ 1.42; National Institutes of Health, Bethesda, MD, USA; https://imagej.nih.gov/ij/). qBEI data of the calcified nidus were compared with those of the trabecular bone by using the Mann–Whitney U test. These data are reported as mean ± SD, while p-values < 0.05 were considered statistically significant.

We additionally measured the diameter of the nidus and the central calcification in the CT images using to integrated tool in the local picture archive and communication system (PACS). This diameter was also quantified from the images obtained by qBEI. The associations between these data were tested using Pearson's correlation analysis. Level of significance was defined as $p < 0.05$.

3. Results

3.1. Case 1: 48-year-old male with subchondral osteoid osteoma of the lateral femur condyle

This patient presented with persistent and non-specific pain in the right knee that he had for over two years. At clinical examination, there was localized pain over the lateral femur condyle. Arthroscopy had been performed elsewhere on the basis of suspected aseptic osteonecrosis/spontaneous osteonecrosis of the knee (SONK). At presentation in our department, MRI showed no articular collapse but persistent bone marrow edema (Fig. 1A). Extended laboratory tests and DXA did not point to any metabolic bone disease with normal bone turnover, vitamin D levels and bone mineral density (Table 1). Since a typical response to salicylates was reported, we initiated an additional thin layer CT scan. Indeed, a nidus with a diameter of 6.5 mm was found (Fig. 1A). At reexamination, the nidus could also be found in one MRI

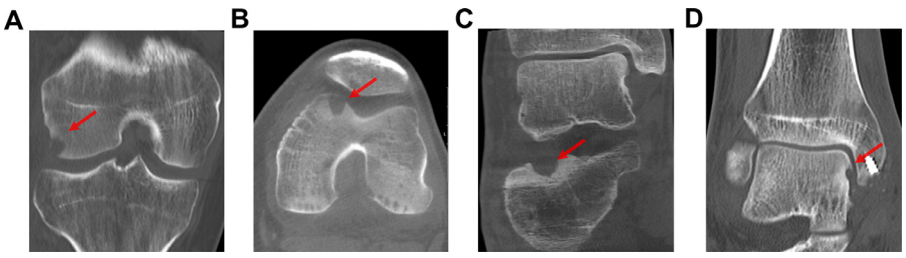

Fig. 2. *Postoperative imaging confirming successful resection.* (A) Postoperative coronal CT reformat in *Case 1* confirming successful resection. (B) Postoperative axial CT reformat in *Case 2*. (C) Postoperative lateral radiograph in *Case 3*. (D) Postoperative coronal CT reformat in *Case 4*.

slice (Fig. 1B). Arthroscopic resection of the tumor was performed. Postoperative CT indicated successful tumor resection (Fig. 2A). Histological analysis confirmed the diagnosis of a subchondral OO. After the surgery, the patient was fully able to walk without any pain.

3.2. Case 2: 26-year-old male with osteoid osteoma of the lateral femur condyle

In this case, unspecific knee pain for more than 2 years responding to ibuprofen was reported. Extensive bone marrow edema of the medial femur condyle was initially detected by MRI (Fig. 1C). Due to persistent edema, core decompression was performed. However, the bone marrow edema persisted thereafter. A CT was performed due to typical medical history (nocturnal pain and response to NSAID) and revealed a small nidus in the anteromedial femur condyle (4.5 mm diameter) that was subsequently also recapitulated on MRI (Fig. 1D). The tumor was resected using intraoperative navigated CT imaging, which confirmed its correct localization (Fig. 2B).

3.3. Case 3: 22-year-old male with osteoid osteoma of the calcaneus

This 22-year old male patient was referred to our outpatient clinic due to severe pain in the right foot which he suffered from for a total of 3 years. Only ibuprofen treatment led to moderate reduction of pain levels. Due to the persistent bone marrow edema syndrome in the calcaneus seen on MRI scans core decompression was performed. Additional CT showed a 4.5 mm nidus in the calcaneus that was localized subchondrally (Fig. 1E) and also seen in MRI scans when re-examining all slices (Fig. 1F). DXA measurements revealed osteopenia in the hip (Table 1). The tumor was successfully resected (Fig. 2C). Histological analysis, again, confirmed the diagnosis of a subchondral OO. After the surgery, the patient was free of pain and after 6 weeks he was fully able to walk and move his foot.

3.4. Case 4: 20-year-old male with osteoid osteoma of the talus

Another patient with persistent pain in the right ankle joint presented at our clinic. On MRI a pronounced bone marrow edema in the talus as well as effusion in the upper ankle joint was seen (Fig. 1G). No signs of an underlying rheumatic disease or bone metabolic disorder were detected by extended laboratory analyses (Table 1). The patient received a single dose of off-label intravenous bisphosphonate (ibandronate), however, no improvements in pain levels could be noted.

Because of the unusual course of the disease and the reported pain response to aspirin, we initiated a CT scan as well as high-resolution peripheral quantitative CT (HR-pQCT). Here, a classical nidus with central calcification was seen (Fig. 1G) and later also confirmed in the initial MRI scan (Fig. 1H). The patient was operated by a specialist foot surgeon, where the tumor was surgically removed (Fig. 2D). The patient was free of pain shortly after the surgery and histological analysis confirmed the diagnosis of subchondral OO.

3.5. Micro-morphological findings

The bone biopsies were further analyzed by detailed undecalcified histology and quantitative backscattered electron imaging (*qBEI*). In fact, the tumor could be readily determined in the macroscopic images of the resection specimens (Fig. 3A). Contact radiography confirmed the radiolucent nidus with a central calcification (Fig. 3B). The nidus area was mirrored by a circular area of unmineralized osteoid with central parts of mineralized tissue as detected in the von Kossa stained histological overview (Fig. 3C). Further histological analyses showed fat cell fragmentation within the bone marrow close to the nidus area indicative of bone marrow edema (Fig. 3D). The tumor itself consisted of structurally disorganized woven bone with >50% non-mineralized osteoid and high numbers of osteoblasts and osteoclasts in all cases (Fig 3E–G). In polarized light microscopy, the tumor presented with disorganized collagen structures compared to well-aligned collagen fibrils in the adjacent trabecular bone (Fig. 3H).

qBEI analysis revealed normally mineralized trabecular bone next to the nidus containing alternating bright and dark areas this indicating a vital remodeling process (Fig. 4A). The calcified part of the nidus (CN) showed different sizes among the cases. Next to a tendency towards higher mean mineralization (CaMean, 24.8 ± 3.2 *vs.* 23.7 ± 0.09 wt %), a significantly higher mineralization heterogeneity (CaWidth, 4.66 ± 0.27 *vs.* 3.46 ± 0.26 wt%) was detected in the calcified nidus compared to the adjacent trabecular bone (Fig. 4B–D). As a result, the bone mineral density distribution (BMDD) curves confirmed the altered mineralization pattern of the calcified nidus (Fig. 4D). Measurements of the diameter of the nidus and the central calcification revealed that the nidus diameter correlated positively with the diameter of the central calcification, while the calcification in CT was also highly correlated with that measured by qBEI (Fig. 4E, F).

4. Discussion

In this study, we have demonstrated extensive bone marrow edema (BME) as an important accompanying aspect of intra-articular OO. Although only performed in a relatively small patient cohort, the subsequent micro-morphological analysis revealed the microstructural basis for the typical MRI and CT appearance of OO, thereby providing the first available data regarding the matrix mineralization of the respective resection specimens using quantitative backscattered electron imaging.

In the clinical part of this study, we studied the potential relationship between peritumoral edema and bone mineral status, which had not been previously assessed. We found that BME was not associated with alterations in the skeletal status or bone metabolism in these patients (e.g., low DXA T-score, altered bone turnover markers) besides low vitamin D levels. In fact, only one patient presented with a low DXA Z-score < −2.0. As certain disorders of bone metabolism (e.g. secondary hyperparathyroidism, increased bone resorption) were previously found in patients with primary BME syndrome [13], it was important for us to exclude metabolic factors that may have aggravated the BME in response to the OO. This also involved the exclusion of mineralization defects of the skeleton that have been associated with bone marrow edema (e.g., osteomalacia due to vitamin D deficiency [13], hypophosphatasia [14]). In our cases, vitamin D deficiencies were balanced with 20,000 IE of cholecalciferol weekly. Since metabolic bone disorders were excluded, it has to be assumed that the OO represents the major stimulus for the development of BME (most likely *via* the production of prostaglandins). Regarding the associations between OO and (local) bone turnover, it is also interesting to note that OO was previously associated with high osteocalcin levels; and OO removal led to a decrease of osteocalcin levels [15]. In contrast, all our OO patients presented with normal osteocalcin levels before tumor resection.

Perinidal or peritumoral edema was previously described in OO [16] and was most pronounced in younger patients with no apparent relation to drug therapy [17–19]. Peritumoral edema was also seen in patients with osteoblastoma [20] and in other tumor entities, where the size of peritumoral bone marrow edema was associated with increased prostaglandin production [21]. In the foot, bone marrow edema was reported as a frequent finding in patients with OO [22]. The patients from this study presented with a bone marrow edema that was not only preinidal, but also more extensive including larger areas of the bone. It is interesting to note that this extensive BME was only seen in patients with intra-articular OO and not in cases of OO affecting the diaphysis of the long bones. Therefore, it remains to be addressed if patients with intra-articular OO are more susceptible to bone marrow edema.

The radiographic description of the nidus as radiolucent with a mineralized center of the nidus was fully recapitulated by the conducted micro-morphological analyses of the resection specimens (i.e.,

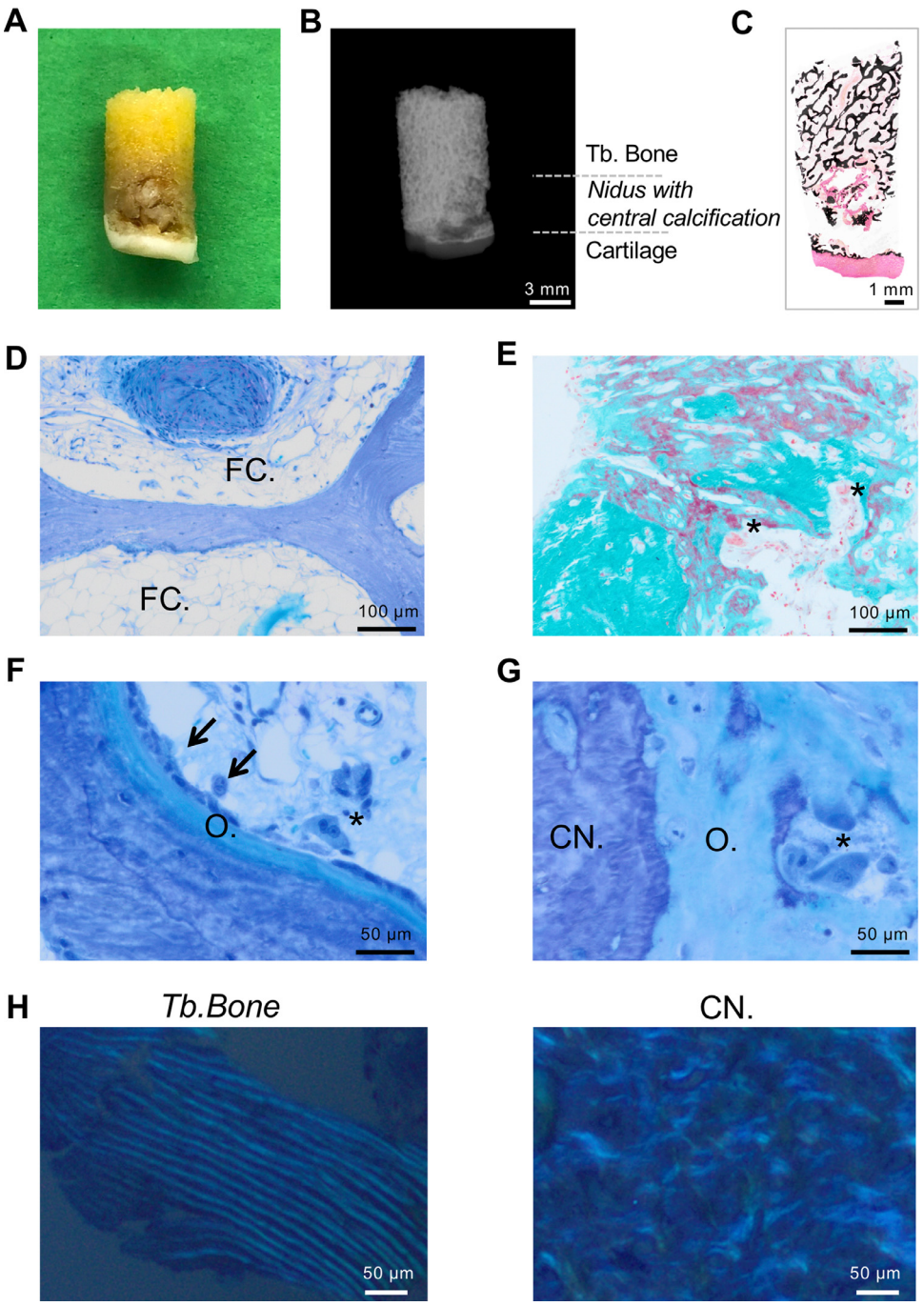

Fig. 3. *Histological findings.* (A) Macroscopic photograph of the core biopsy of *Case 2*. (B) Corresponding contact radiography in which the nidus can readily be determined. (C) Overview of an undecalcified processed resection specimen reveals subchondral hyperosteoidosis. Von Kossa staining. (D) Intertrabecular fatty bone marrow with moderate edema surrounding the fat cells (FC.) and artery (top). (E) Immature sclerotic woven bone with osteoid and resorption lacunae with increased osteoclast indices (asterisks). (F) Area of trabecular bone next to the tumor showing active bone remodeling. Osteoblasts (arrow), osteoclasts (asterisk) and osteoid (O.). (G) Interface between the calcified nidus (CN.) and the surrounding osteoid mass (O.), Osteoclasts (asterisk). Toluidine blue or trichrome Masson–Goldner staining. (H) Polarized light microscopy indicating the disorganized collagen alignment within the calcified nidus.

undecalcified histology, qBEI). Specifically, we found osteoid accumulation together with a highly and heterogeneously mineralized matrix mineralization in the center of the nidus compared to the surrounding trabecular bone. The presence of higher mineralization heterogeneity could be due to lower matrix mineralization in the outer areas of the nidus as well as poor bone remodeling with subsequent central hypermineralization, since bone that is covered by large surfaces of osteoid cannot be resorbed by osteoclasts. Similarly, hypermineralization of osteoid-framed bone was previously shown in vitamin D deficiency [23]. Higher mineralization heterogeneity was also detected in patients with hypophosphatasia [24].

Considering all diagnostic options, CT imaging represents the most specific technique to detect OO [1,25,26], especially as a tumor size of under 3 mm may lead to misinterpretation of MRI images [3,26]. In general, reliance on MR imaging alone was previously found to lead to misdiagnosis [2,27]. Nonetheless, MRI may also be helpful in some cases. Especially in noncortical lesions with little periosteal reaction such as intra-articular OO), demarcation of the nidus within the bone marrow edema could facilitate the diagnostic process [17]. In this context, it was previously questioned whether bone marrow edema or the nidus arises first [28]. In the femoral neck, a half-moon appearance of bone marrow edema (i.e., “half-moon sign”) has been described as a highly sensitive and specific sign for the diagnosis of osteoid osteoma [11]. Although no specific BME pattern could be observed in our cases, the nidus was confirmed at reexamination of MRI scans. However, BME was the reason for a number of incorrect diagnoses and various surgical treatments such as core decompression. Therefore, it was essential to evaluate the patients’ medical history including their pain characteristics. These cases indicate that if nocturnal pain and NSAID sensitivity are present, CT should be performed in addition to MRI to confirm the

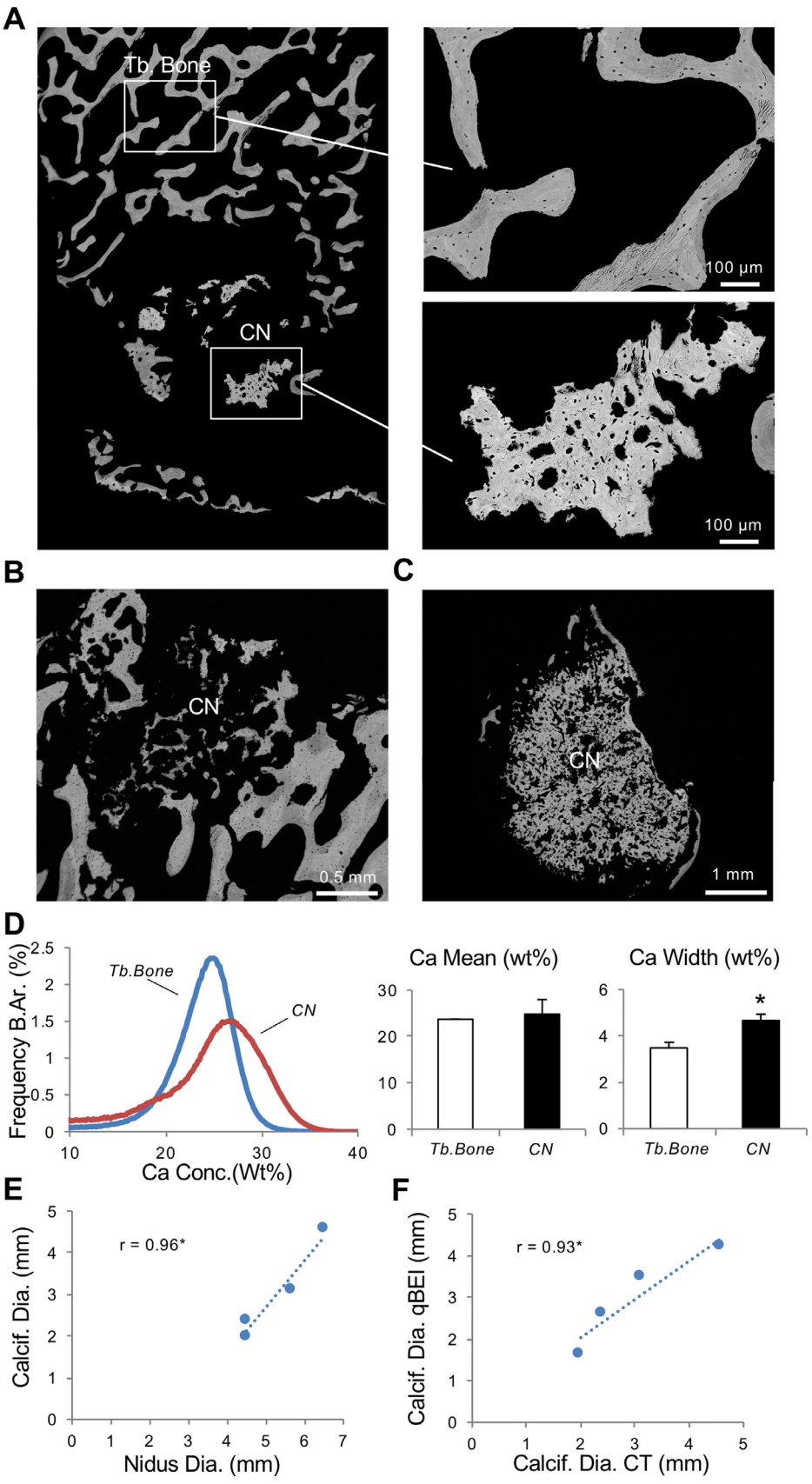

Fig. 4. *Bone mineral density distribution of the calcified nidus assessed by quantitative backscattered electron imaging (qBEI).* (A) Exemplary image of the analyzed area (*Case 2*). Insets: trabecular bone (Tb. Bone, top) and calcified nidus (CN, bottom). (B,C) qBEI analysis revealed calcified nidus areas of different sizes (B) *Case 3*, (C) *Case 4*. (D) BMDD curves showing significantly higher mineralization heterogeneity (CaWidth) and equal mean mineralization values (CaMean) for the calcified nidus compared to the adjacent trabecular bone. (E) Correlation analysis of nidus diameter and nidus calcification diameter *via* CT, and (F) calcification diameter *via* CT and calcification diameter *via* qBEI. $*p < 0.05$.

suspect of OO.

Regarding treatment options, bisphosphonates were found to be effective in pain level reduction [29]. This was associated with bone marrow edema attenuation, which is most definitely a major reason for pain improvements. Consistently, bisphosphonates and denosumab were found effective in the treatment of BME [30,31]. Nonetheless, sustained success can only be reached by a complete removal of the tumors, which is why the surgical resection therefore remains the treatment of first choice in most cases. In line with previous observations [32] we histologically detected nerve fibers in the bone adjacent to the nidus, which fits to the peculiar pain history of patients with OO. The limitations of our study include the fact that only four patients could be analyzed in detail, which hinders possible statements on statistical significance. Furthermore, we were not able to assess all patients at follow-up, which is why no statement regarding the development of laboratory values (e.g., osteocalcin) following tumor resection can be made.

Taken together, we have demonstrated that extensive bone marrow edema can mask osteoid osteoma, leading to delayed diagnosis. While it is essential to identify the atypical cases of osteoid osteoma as a differential diagnosis to musculoskeletal pain, certain patterns of impaired bone mineral status could not be confirmed in these patients. Next to a detailed clinical workup, our study revealed the micro-morphological characteristics of osteoid osteoma specimens demonstrating a heterogeneously mineralized bone material within the non-mineralized nidus, which explains the frequent description of a central calcification within the nidus in conventional imaging.

Declaration of Competing Interest

All authors declare that they have no conflict of interest.

Funding

T.R. is supported by the German Research Foundation under Grant no. RO 5925/1-1.

Compliance with ethical standards

All procedures performed in studies involving human participants were in accordance with the ethical standards of the institutional and/or national research committee and with the 1964 Helsinki declaration and its later amendments or comparable ethical standards. For this type of study formal consent is not required. Informed consent was obtained from all individual participants included in the study.

References

[1] J. Assoun, G. Richardi, J.J. Railhac, C. Baunin, P. Fajadet, J. Giron, P. Maquin, J. Haddad, P. Bonnevialle, Osteoid osteoma: MR imaging versus CT, Radiology 191 (1) (1994) 217–223.
[2] M. Krause, R. Oheim, N.M. Meenen, K.H. Frosch, M. Amling, Intra-articular osteoid osteoma in the proximal tibia and its imaging characteristics, Knee 23 (5) (2016) 915–919.
[3] T. Rolvien, J. Zustin, H. Mussawy, T. Schmidt, P. Pogoda, P. Ueblacker, Intra-articular osteoid osteoma as a differential diagnosis of diffuse mono-articular joint pain, BMC Musculoskelet. Disord. 17 (1) (2016) 455.
[4] L. Matthies, T. Rolvien, T.J. Pakusa, C. Knipfer, M. Gosau, M. Amling, R.E. Friedrich, J. Zustin, Osteoid osteoma of the mandible - Clinical and histological findings, Anticancer Res. 39 (1) (2019) 291–296.
[5] J. Edeiken, A.F. DePalma, P.J. Hodes, Osteoid osteoma. (Roentgenographic emphasis), Clin. Orthop. Relat. Res. 49 (1966) 201–206.
[6] P.J. Boscainos, G.R. Cousins, R. Kulshreshtha, T.B. Oliver, P.J. Papagelopoulos, Osteoid osteoma, Orthopedics 36 (10) (2013) 792–800.
[7] M.W. Fittall, W. Mifsud, N. Pillay, H. Ye, A.C. Strobl, A. Verfaillie, J. Demeulemeester, L. Zhang, F. Berisha, M. Tarabichi, M.D. Young, E. Miranda, P.S. Tarpey, R. Tirabosco, F. Amary, A.E. Grigoriadis, M.R. Stratton, P. Van Loo, C.R. Antonescu, P.J. Campbell, A.M. Flanagan, S. Behjati, Recurrent rearrangements of FOS and FOSB define osteoblastoma, Nat. Commun. 9 (1) (2018) 2150.
[8] D. Baumhoer, F. Amary, A.M. Flanagan, An update of molecular pathology of bone tumors. Lessons learned from investigating samples by next generation sequencing, Genes Chromosomes Cancer 58 (2) (2019) 88–99.
[9] A.F. Mavrogenis, R. Dimitriou, I.S. Benetos, D.S. Korres, P.J. Papagelopoulos, Juxta-articular osteoid osteoma of the talar neck: a case report, Clin. Podiatr. Med. Surg. 27 (4) (2010) 629–634.
[10] H. He, H. Xu, H. Lu, Y. Dang, W. Huang, Q. Zhang, A misdiagnosed case of osteoid osteoma of the talus: a case report and literature review, BMC Musculoskelet. Disord. 18 (1) (2017) 35.
[11] M.E. Klontzas, A.H. Zibis, A.H. Karantanas, Osteoid osteoma of the femoral neck: use of the half-moon sign in MRI diagnosis, AJR Am. J. Roentgenol. 205 (2) (2015) 353–357.
[12] T. Koehne, E. Vettorazzi, N. Kusters, R. Luneburg, B. Kahl-Nieke, K. Puschel, M. Amling, B. Busse, Trends in trabecular architecture and bone mineral density distribution in 152 individuals aged 30-90 years, Bone 66 (2014) 31–38.
[13] N. Oehler, H. Mussawy, T. Schmidt, T. Rolvien, F. Barvencik, Identification of vitamin D and other bone metabolism parameters as risk factors for primary bone marrow oedema syndrome, BMC Musculoskelet. Disord. 19 (1) (2018) 451.
[14] T. Schmidt, H. Mussawy, T. Rolvien, T. Hawellek, J. Hubert, W. Ruther, M. Amling, F. Barvencik, Clinical, radiographic and biochemical characteristics of adult hypophosphatasia, Osteoporos. Int. 28 (9) (2017) 2653–2662.
[15] C.B. Confavreux, O. Borel, F. Lee, G. Vaz, M. Guyard, C. Fadat, M.C. Carlier, R. Chapurlat, G. Karsenty, Osteoid osteoma is an osteocalcinoma affecting glucose metabolism, Osteoporos. Int. 23 (5) (2012) 1645–1650.
[16] J.W. Chai, S.H. Hong, J.-Y. Choi, Y.H. Koh, J.W. Lee, J.-A. Choi, H.S. Kang, Radiologic diagnosis of osteoid osteoma: from simple to challenging findings, Radiographics 30 (3) (2010) 737–749.
[17] A.R. Spouge, L.M. Thain, Osteoid osteoma: MR imaging revisited, Clin. Imaging 24 (1) (2000) 19–27.
[18] S. Ehara, D.I. Rosenthal, J. Aoki, K. Fukuda, H. Sugimoto, H. Mizutani, K. Okada, M. Hatori, M. Abe, Peritumoral edema in osteoid osteoma on magnetic resonance imaging, Skeletal Radiol. 28 (5) (1999) 265–270.
[19] A.B. Goldman, R. Schneider, H. Pavlov, Osteoid osteomas of the femoral neck: report of four cases evaluated with isotopic bone scanning, CT, and MR imaging, Radiology 186 (1) (1993) 227–232.
[20] S.L. James, D.M. Panicek, A.M. Davies, Bone marrow oedema associated with benign and malignant bone tumours, Eur. J. Radiol. 67 (1) (2008) 11–21.
[21] S. Yamamura, K. Sato, H. Sugiura, H. Katagiri, Y. Ando, H. Fukatsu, H. Iwata, Prostaglandin levels of primary bone tumor tissues correlate with peritumoral edema demonstrated by magnetic resonance imaging, Cancer 79 (2) (1997) 255–261.
[22] S. Shukla, A.W. Clarke, A. Saifuddin, Imaging features of foot osteoid osteoma, Skeletal Radiol. 39 (7) (2010) 683–689.
[23] B. Busse, H.A. Bale, E.A. Zimmermann, B. Panganiban, H.D. Barth, A. Carriero, E. Vettorazzi, J. Zustin, M. Hahn, J.W. Ager 3rd, K. Puschel, M. Amling, R.O. Ritchie, Vitamin d deficiency induces early signs of aging in human bone, increasing the risk of fracture, Sci. Transl. Med. 5 (193) (2013) 193ra88.
[24] T. Rolvien, T. Schmidt, F.N. Schmidt, S. von Kroge, B. Busse, M. Amling, F. Barvencik, Recovery of bone mineralization and quality during asfotase alfa treatment in an adult patient with infantile-onset hypophosphatasia, Bone 127 (2019) 67–74, https://doi.org/10.1016/j.bone.2019.05.036 [Epub ahead of print].
[25] M. Harun, Y. Hayrettin, M. Serhat, C. Engin, C. Kamil, A. Armagan, P.A. Sancar, Atypical location of an osteoid osteoma with atypical anterior knee pain, Int. J. Surg. Case Rep. 5 (11) (2014) 873–876.
[26] C. Pikoulas, G. Mantzikopoulos, L. Thanos, D. Passomenos, C. Dalamarinis, K. Glampedaki-Dagianta, Unusually located osteoid osteomas, Eur. J. Radiol. 20 (2) (1995) 120–125.
[27] M. Davies, V.N. Cassar-Pullicino, M.A. Davies, I.W. McCall, P.N. Tyrrell, The diagnostic accuracy of MR imaging in osteoid osteoma, Skelet. Radiol. 31 (10) (2002) 559–569.
[28] E. Uygur, O. Poyanlı, O. Kılıçoğlu, Which emerges first: bone marrow edema or nidus in osteoid osteoma? J. Am. Podiatr. Med. Assoc. 108 (6) (2018) 523–527.
[29] V. Bousson, T. Leturcq, H.K. Ea, O. Hauger, N. Mehsen-Cetre, B. Hamze, C. Parlier-Cuau, J.D. Laredo, T. Schaeverbeke, P. Orcel, An open-label, prospective, observational study of the efficacy of bisphosphonate therapy for painful osteoid osteoma, Eur. Radiol. 28 (2) (2018) 478–486.
[30] M.J. Simon, F. Barvencik, M. Luttke, M. Amling, H.W. Mueller-Wohlfahrt, P. Ueblacker, Intravenous bisphosphonates and vitamin D in the treatment of bone marrow oedema in professional athletes, Injury 45 (6) (2014) 981–987.
[31] T. Rolvien, T. Schmidt, F. Barvencik, M. Amling, Denosumab in bone marrow oedema syndrome. response to letter to the editor of injury, Injury 48 (10) (2017) 2368.
[32] J.X. O'Connell, S.S. Nanthakumar, G.P. Nielsen, A.E. Rosenberg, Osteoid osteoma: the uniquely innervated bone tumor, Mod. Pathol.: Off. J. U. S.Can. Acad. Pathol., Inc 11 (2) (1998) 175–180.